Journal of Alloys and Compounds, 188 (1992) 36–41
JALCOM 9005

Monovalent copper in insulators

G. Le Flem
Laboratoire de Chimie du Solide du CNRS, 351 cours de la Libération, 33405 Talence (France)

Abstract

The crystal chemistry of monovalent copper in insulators is characterized by two trends: a more or less linear coordination by the ligands and the formation of copper aggregates. Recent spectroscopic investigations illustrate clearly the influence of these structural features on the luminescence properties.

1. Introduction

At first sight the electronic d^{10} configuration of Cu^+ can be considered as exhibiting a spherical shape. Nevertheless, the Cu(I) crystal chemistry of insulators is mostly characterized by two trends: a more or less linear coordination by ligands and the formation of a cluster-like assembly [1]. Such aggregates are observed in coordination compounds as well as in inorganic solid-state materials.

The luminescent investigations of compounds containing various proportions of Cu^+ ions illustrate clearly the influence of these structural features on the optical properties, and allow us to postulate a phenomenological model describing the spectroscopy of these various Cu(I) emitting centres.

The first part of this paper reviews recent publications describing the structure of Cu(I) rich insulators. The case of $CuZr_2(PO_4)_3$ and its related compounds will be discussed extensively as examples of oxides containing both isolated Cu^+ ions and Cu^+–Cu^+ pairs. The second part analyses the most recent data related to Cu(I) luminescence for various types of materials in order to suggest a model based on the coupling between Cu^+ excited states and the highest phonon energy of the lattice.

1.1. Cu(I) in a linear environment

Beyond the classical case of Cu_2O, the delafossite cuprous oxides $BCuO_2$ (B is a trivalent ion with various ionic sizes) is representative of the linear coordination of Cu^+ ions in oxides [2]. In addition to this twofold coordination by oxygen, this cation is surrounded by six other copper ions hexagonally arranged in the basal plane perpendicular to the O–Cu–O axis (Fig. 1). Cu luminescence can be observed as B in a rare earth element like lanthanum [3] or yttrium [4].

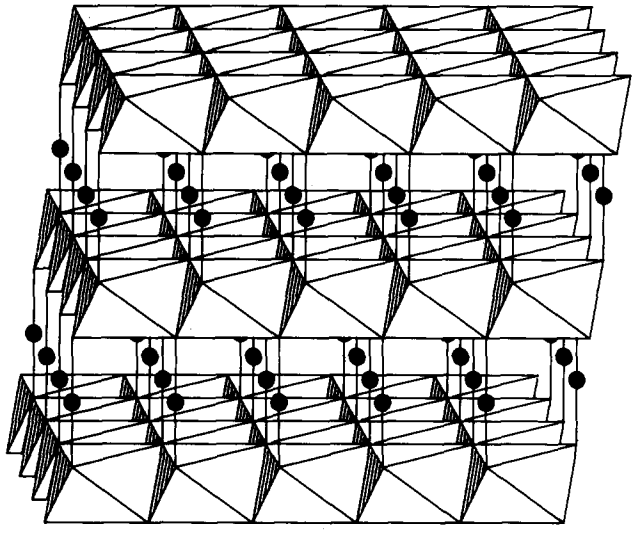

Fig. 1. Delafossite type structure: solid black circles represent the Cu atoms.

Cherry red crystals of composition $Cu(I)NbO_3$ were recently prepared by Marinder and Wahlstrom [5]. The crystal structure can be compared with that of delafossite: there is an identical oxygen environment for the Cu and for the counter-cation. The main difference is the staircase-like layers of the Nb_4O_{16} groups existing in the niobate. By increasing the proportion of niobium, *e.g.* in $CuNb_{13}O_{33}$ [6], the irregular (NbO_6) octahedra share corners and/or edges in a three-dimensional framework but the Cu atoms remain coordinated to two oxygen atoms in a linear geometry.

This dumbbell-like geometry of (CuO_2) groups was also found in a white compound such as $SrCu_2O_2$ [7].

In all these structural types the Cu–O distances are included between 1.79 and 1.90 Å.

0925-8388/92/$5.00

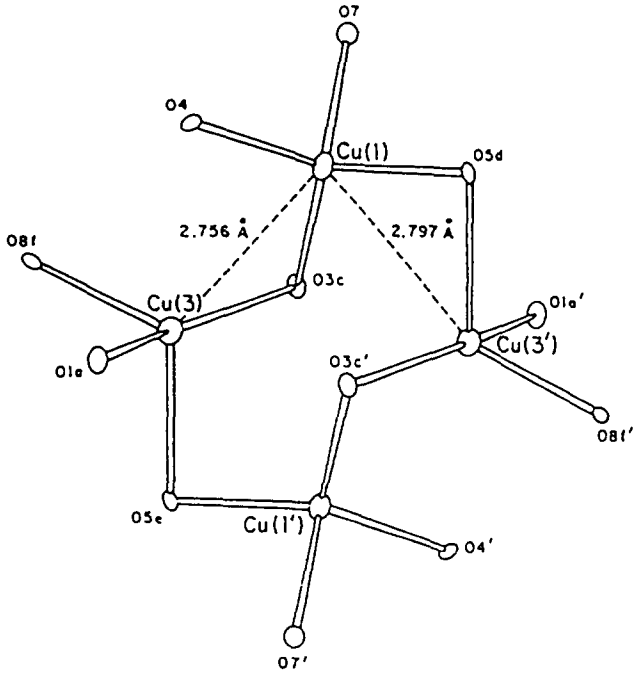

Fig. 2. Details of the tetrameric CuO_4 units in $Cu_6Mo_5O_{18}$ emphasizing the short Cu–Cu interatomic distance [9].

1.2. Cu(I) in a non-linear environment

A Cu(I) non-linear environment can be illustrated by the structure of two rich Cu molybdates $Cu_4Mo_5O_{17}$ and $Cu_6Mo_5O_{18}$ recently reported by McCarron and Calabrese [8, 9]. The structure of the first compound involves four independent Cu oxide polyhedra: three tetahedra and one pseudo-octahedron, in reality a linear coordination with two short Cu–O distances (1.94 Å) and four longer ones (2.30 Å). In the tetrahedral groups the Cu–O distances are distributed between 1.918 and 2.161 Å. Similar CuO_4 groups exist in the lattice of $Cu_6Mo_5O_{18}$ (1.905 Å $< d <$ 2.148 Å). Some of these entities are arranged in tetrameric units (Fig. 2) where the Cu–Cu distance is only 0.2 Å longer than the Cu–Cu distance of 2.56 Å found in Cu metal. This is the first example of a Cu aggregate identified in an oxide system for inorganic materials.

1.3. Cu(I) in aggregates

Unusually short intermetallic distances are found particularly in organo-Cu(I) compounds. The most simple is the cuprous acetate, which has a two-dimensional structure consisting of infinite planar chains of binuclear dimeric units $Cu_2(O_2CCH_3)_2$ [10]. These units are bridged by Cu and O atoms to form the polymer (Fig. 3). Each Cu atom is coordinated to three O atoms and one Cu atom. Two of these O atoms are 1.91 Å distant but the third O atom located in the adjacent eight-membered ring system is 2.31 Å away. In this structure a short Cu–Cu distance of 2.56 Å still exists.

Other examples of Cu aggregates observed in coordination compounds have been reviewed by Jansen [1].

Rath *et al.* [11] have reported several crystal structures of Cu(I) iodide complexes with Cu iodide entities of various structural formats and short Cu–Cu distances. Such clusters could be a new type of emitting centre.

This assumption was strongly corroborated by the study of the relationship between the structure and luminescent properties of $CuZr_2(PO_4)_3$ and its related compounds.

1.4. The structures of $CuZr_2(PO_4)_3$ and related compounds

$CuZr_2(PO_4)_3$ is of the Nasicon structural type [12]. The lattice consists of a three-dimensional network made up of PO_4 tetrahedra sharing corners with ZrO_6 octahedra. Cu is located in an elongated antiprism usually labelled M1 sharing common faces with two (ZrO_6) octahedra along the c axis. The Cu atoms are actually distributed between six off-centre equivalent positions with a statistical occupancy (1/6) (Fig. 4).

A similar cationic distribution was also found for $CuTi_2(PO_4)_3$ [13]. In both cases, the Cu environment is characterized by two short distances ($d_{Cu\ O} < 2.06$ Å) and four larger distances of more than 2.50 Å: the linking of Cu by O appears to be a compromise between the linear coordination and the geometry of the M(1) site created by the covalent network.

The distance between the symmetrical positions of Cu in M1 is very small in the case of $CuTi_2(PO_4)_3$ (1.59 Å) but noticeably larger for the zirconium phosphate (2.25 Å from X-ray diffraction).

X-ray absorption spectroscopy has been used to characterize the local order around Cu atoms. The formation of Cu pairs in M1 was evidenced only for $CuZr_2(PO_4)_3$ with a Cu–Cu distance of 2.40 Å. In contrast, the smaller size of the M1 site of $CuTi_2(PO_4)_3$ prevents the formation of such clusters [14]. A similar Cu environment and Cu pairing were also found in the structure of the related phosphates ($H_{0.5}Cu_{0.5}Zr_2(PO_4)_3$ and $Cu_2CrZr(PO_4)_3$ [14, 15]. The formation of such pairs is induced by the large volume of the M1 site and their environment differs from that usually observed in organometallic compounds or in $Cu_6Mo_5O_{18}$ in that it lacks a ligand bridge between the two metallic ions.

2. Luminescence of Cu(I) insulators: an overview

The luminescence of Cu^+ ion in insulators was first reported for Cu phosphates with high luminescence efficiency [16, 17]. In the last decades several studies have been devoted to fundamental aspects of Cu^+ luminescence in rock salt lattices which can be considered as model systems [18–23].

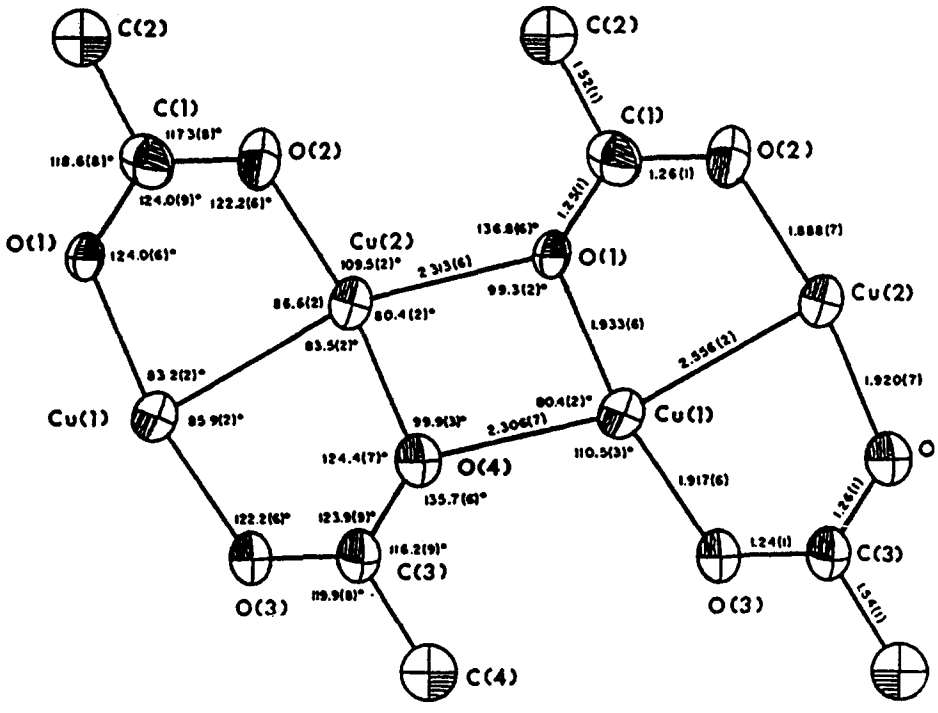

Fig. 3. The structure of $Cu(O_2CCH_3)$ [10].

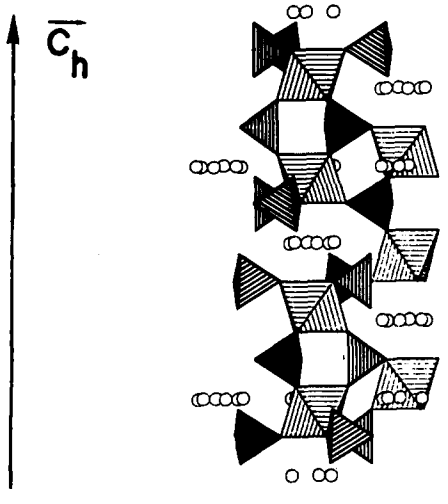

Fig. 4. Details of the structure of $CuZr_2(PO_4)_3$; circles represent the Cu atoms within the M1 site [12].

The recent discovery of new Cu rich luminescent oxides $CuZr_2(PO_4)_3$ [24] and $CuLaO_2$ [3], and their related compounds, has led to a discussion of the influence of Cu environment by ligand or of Cu aggregation on the spectroscopic properties. These studies have looked at solid-state inorganic materials as well as coordination compounds. However, the need for tuneable laser or white emitting phosphors has accentuated the necessity of considering the case of Cu doped glass.

2.1. Cu(I) in rock salt crystals

The ground state of Cu^+ has an electronic configuration $1s^22s^22p^63s^23p^63d^{10}$. In an octahedral crystal field the d states are split into triply degenerate components t_{2g} and doubly degenerate components e_g. Only the $3d^{10} \rightarrow 3d^9\,4s$ and $3d^{10} \rightarrow 3d^9\,4p$ transitions have to be considered. The former are forbidden by the parity rules. However, lattice vibration can mix states of odd parity into the even parity states making these transitions partially allowed. Assuming Cu^+ located at the centre of the octahedral site (Cu^+ in NaF, LiCl, NaCl) the main absorption bands are assigned to the transition $^1A_{1g} \rightarrow {}^1E_g$, $^1A_{1g} \rightarrow {}^1T_{2g}$ ($3d^94s$) and $^1A_{1g} \rightarrow {}^3T_u$, $^1A_{1g} \rightarrow {}^1T_u$ ($3d^94p$). The emission comes from the lowest excited state ^3E_g which is split in two very close levels T_{2g} and T_{1g} by the spin orbit interaction. Such excited-state energy distribution explains the strong temperature dependence of the fluorescence decay, which is described by the rate equation

$$\tau^{-1} = [A_{31} + A_{21} \exp(-\epsilon/kT)]/[1 + \exp(\epsilon/kT)] \qquad (1)$$

where A_{31} and A_{21} are the radiative transitions between the excited states (upper level 2 and lower level 3) and the ground state. ϵ represents the energy mismatch between the two excited states. Table 1 gives the energies of excitation and emission in various Cu doped alkali halides [21]. The emission is always located in the UV range. In all cases an increase in the $3d \rightarrow 4s$ transition energies and a decrease in the $3d \rightarrow 4p$ transition energies

TABLE 1. Excitation and emission transition energies in various alkali halides [21]

Cu⁺ in	$d^{10} \rightarrow d^9s$ transitions			$d^{10} \rightarrow d^9p$ transitions	
	Emission	Excitation	Excitation	Excitation	Excitation
	$^3E_g \rightarrow {}^1A_{1g}$	$^1A_{1g} \rightarrow {}^1E_g$	$^1A_{1g} \rightarrow {}^1T_{2g}$	$^1A_{1g} \rightarrow {}^3T_u$	$^1A_{1g} \rightarrow {}^1T_u$
NaF	26670 (375 nm)	31700 (315 nm)	35700 (280 nm)	59800 (167 nm)	60000 (167 nm)
LiCl	31250 (320 nm)	38700 (258 nm)	42400 (236 nm)	55700–59400 (179–168 nm)	57500 (174 nm)
NaCl	28570 (350 nm)	35200 (284 nm)	38500 (260 nm)	56900 (175 nm)	58800 (170 nm)

is observed in the impure crystal over the corresponding free transitions.

As the size of the octahedral site increases, *e.g.* in KCl:Cu^+, KBr:Cu^+ and KI:Cu^+ the $3d^{10} \rightarrow 3d^94s$ transitions are allowed mainly by displacement of Cu^+ in an off-centre position [22, 23].

2.2. Cu(I) luminescence in Cu(I) rich oxides

2.2.1. Cu(I) in linear environment: $LaCuO_2$ [3]

Two emission bands were found centred at 550 and 600 nm. The red emission is characterized by a larger Stokes shift than the green emission. As previously mentioned, only one type of site is available for Cu^+ and any perturbation of sites by a neighbouring Cu^{2+} must be disregarded as no Cu^{2+} could be detected by electron paramagnetic resonance (EPR). Therefore the double luminescence of $LaCuO_2$ has been analysed in the context of two types of emission previously described for Cu^+:

(i) α: A "normal" green emission: the emitting levels belong to the $3d^94s$ configuration.

(ii) β: An "extra" red emission which is assumed to result from creation of exciton below the lowest state of the $3d^94s$ configuration. The charge variation of this emitting level induces a negative Stokes shift larger than for the normal emission. Figure 5 illustrates the formation of localized (L) and excitonic (E) excited states in $LaCuO_2$.

2.2.2. The luminescence of $CuZr_2(PO_4)_3$ [25]

Under 254 nm excitation, $CuZr_2(PO_4)_3$ exhibits a violet emission ($\lambda_{max} = 410$ nm) at 6.5 K as well as a green emission peaking at about 550 nm. Above 150 K the green band intensity increases at the expense of the violet, which disappears completely at 230 K. At 300 K $CuZr_2(PO_4)_3$ exhibits the green fluorescence only.

Under 320 nm excitation, the violet emission is never observed. In contrast, at 6.5 K a new band peaking at 460 nm exists in addition to the green one with a comparable high intensity. At 40 K the green fluorescence increases while the blue decreases.

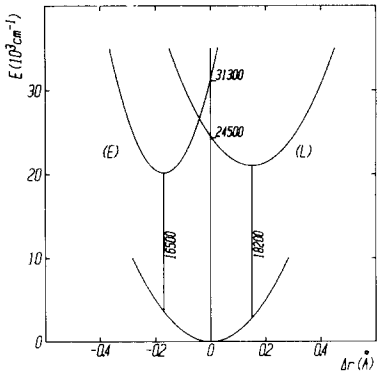

Fig. 5. Configuration coordinate model illustrating the formation of localized (L) and excitonic (E) states in $LaCuO_2$ [3].

Only the thermal evolution of the violet emission lifetime can be described by eqn. (1) with $A_{31} = 5920\ s^{-1}$, $A_{21} = 57140\ s^{-1}$ and $\epsilon = 31\ cm^{-1}$. Therefore this emission can be attributed to a $3d^94s \rightarrow 3d^{10}$ transition of single Cu^+ within the M1 site. A more complete identification of the emitting levels becomes complicated with the off-centre position of Cu^+.

The green emission is characterized by:

(i) A lowering of both excitation and emission energies by about $7000\ cm^{-1}$.

(ii) A larger Stokes shift involving a wider electronic delocalization and a longer lifetime in the explored temperature range.

A similar dynamic evolution has been reported for the white emission of the Cu^+ dimers in $SrCl_2$ [26] and for the green emission of the Cu^+–Cu^+ pairs in Cu(I) doped $Na^+\beta''$ alumina [27].

Accordingly the green emission can be attributed to the $(Cu^+)_2$ dimers existing in the M1 site. This result is consistent with the possibility of Cu(I) pairing predicted by means of molecular orbital calculations [28].

In this model, the emission transition is assumed to occur between a σ bonding orbital created by the two 4s orbitals and the σ^* antibonding orbital derived from the 3d atomic orbital.

Above 150 K a $Cu^+ \rightarrow (Cu^+)_2$ transfer is thermally activated and at room temperature its efficiency is quite high since a large proportion of the green emitters are excited by the violet ones.

The origin of the blue luminescence remains an open question. Its very short lifetime (40 ns) and its very low quenching temperature could be explained by the formation of a Cu^+-Cu^0 pair assuming a very small proportion of Cu^{2+} in the sample. In such a pair the energy level diagram of the $(Cu^+)_2$ system is modified by addition of an electron in the bonding molecular orbital (4s) which corresponds to a stabilization of the cluster.

2.2.3. Cu(I) luminescence in coordination compounds

Several Cu(I) coordination compounds are luminescent but their optical properties have not been yet extensively investigated [29, 30]. Nevertheless in the case of iodide complexes the existence of interacting Cu emitting centres is raised since emission at low energy (550–630 nm) is generally found as Cu–Cu distances are lower than 2.8 Å [11].

2.3. Cu(I) luminescence in glass

When embedded in glass monovalent Cu ions usually give rise to rather strong luminescence [31, 32]. Laser achievement has also been reported [32].

The fluorescence spectrum usually consists of a very broad band covering the whole visible range. As in the case of isolated Cu^+ in crystals, the decays show a strong temperature dependence which can be described by the rate eqn. (1). Several data are listed in Table 2. The values of the different parameters are close to those obtained in crystals. Time-resolved spectroscopy evidences a typical multisite structure: the impurity resides in a large variety of sites and the energy of the various ionic levels may differ substantially. For instance, in the case of the borate described in [33] the emission band, time resolved a short time (100 ns) after the laser excitation pulse, is centred in the blue region and the band is red-shifted as the gate opening delay increases. At the same time, a narrowing of the emission band is actually observed (Fig. 6).

Moreover, Cu pair emitting centres were unambiguously detected in phosphate glass [34]. Two fluorescence bands were simultaneously observed: a unique blue emission exists for low Cu concentration; the thermal dependence of its lifetime can be described by the three-level system (eqn. (1)). In addition, as the Cu concentration increases a red emission appears whose intensity progressively grows at the expense of the blue. Its characteristics are typical of $(Cu^+)_2$ centres.

TABLE 2. Parameters of Cu(I) emission in glasses (eqn. (1))

Materials	A_{31} (s^{-1})	A_{21} (s^{-1})	Σ (cm^{-1})
Phosphate glass: blue emission [34]	4270	42000	15
Borate glass [33]	2247	28300	32
Borate glass [35]	2288	29412	13

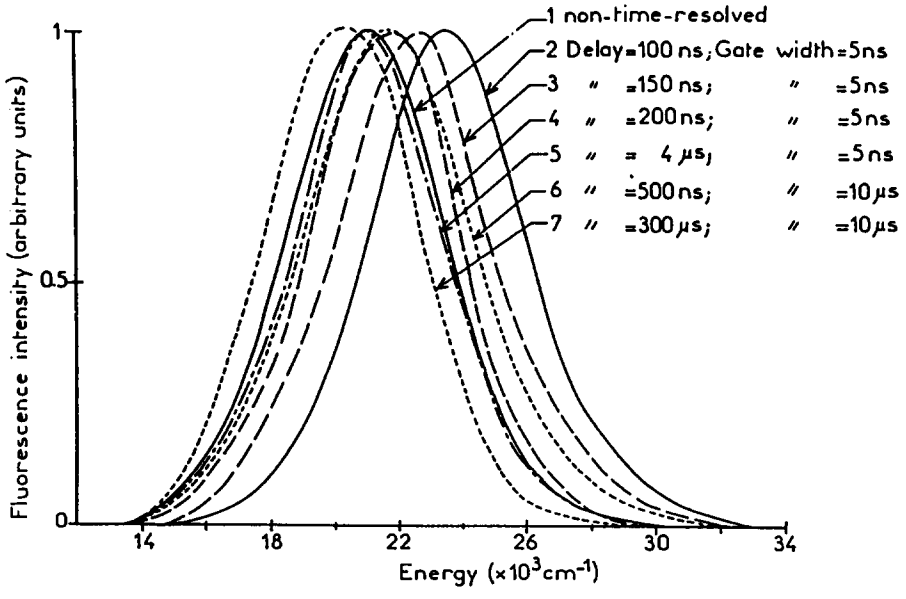

Fig. 6. Time-resolved fluorescence spectra of Cu(I) doped borate under laser excitation at 290 nm ($T = 5$ K) [33].

TABLE 3. Stokes shift (cm^{-1}) of Cu(I) luminescence in various host lattices

	(a) single Cu^+	(b) Copper pairing
SrB_4O_7 [35]	400	
NaF [21]	5500	
NaCl [36]	6700	
$LaCuO_2$ [3]	7000	
Na^+ β'' alumina [27]	10000	15100
NaI [37]	12000	
$CuZr_2(PO_4)_3$ [25]	13300	14000
Borate glass [32]	16700	
Phosphate glass [34]	18100	14300

3. Conclusions

The relationship between the structure of Cu insulators and their luminescent properties can be explained by considering two different situations, depending on whether the Cu ions are isolated or aggregated. Two typical evolutions result from examination of the Stokes shift values in the materials investigated (Table 3).

3.1. Isolated Cu

For all compounds except SrB_2O_4, which has a rigid skeleton [35], the Stokes shift is higher for oxides than for alkali halides. It is enhanced:

(i) By introduction of structural groups exhibiting high energy phonon (*e.g.* phosphate).

(ii) If Cu^+ is located in an off-centre position of a large site (*e.g.* KF compared to NaF).

(iii) In the case of glass which possesses a less compact network than crystals.

The three-level system (eqn. (1)) is able to describe the thermal variation of the emission decay.

3.2. Cu pairs

In contrast, Cu pairing induces an approximately constant Stokes shift value whatever the type of host, crystal or glass. This very surprising result bears witness to the existence of an almost identical emitting centre, *i.e.* aggregates with quasi-constant Cu–Cu distances.

References

1 M. Jansen, *Angew. Chem., Int. Ed. Engl., 26* (1987) 1098.
2 D. B. Rogers, R. D. Shannon, C. T. Prewitt and J. L. Gillson, *Inorg. Chem., 10* (1971) 723.
3 J. P. Doumerc, C. Parent, J. C. Zhang, G. Le Flem and A. Ammar, *C.R. Acad. Sci. Paris, 306* (1982) 1431.
4 P. Boutinaud, Thesis, University of Bordeaux I, 1991.
5 B. O. Marinder and E. Wahlstrom, *Chem. Scr., 23* (1984) 157.
6 F. A. Cotton and R. W. Sandor, *Eur. J. Solid State Inorg. Chem., 25* (1988) 637.
7 C. L. Teske and H. Muller-Buschbaum, *Z. Anorg. Alg. Chem., 379* (2) (1974) 113.
8 E. M. McCarron III and J. C. Calabrese, *J. Solid State Chem., 62* (1986) 64.
9 E. M. McCarron III and J. C. Calabrese, *J. Solid State Chem., 65* (1986) 215.
10 R. D. Mounts, T. Ogura and Q. Fernando, *Inorg. Chem., 13* (4) (1974) 802.
11 N. Rath, E. Holt and K. Tanimura, *Inorg. Chem., 24* (1985) 3934.
12 I. Bussereau, M. B. Belkiria, P. Gravereau, A. Boireau, J. L. Soubeyroux, R. Olazcuaga and G. Le Flem, *Acta Crystallogr.*, in the press.
13 E. M. Carron, J. L. Calabrese and M. B. Subramanian, *Mater. Res. Bull., 22* (1987) 1421.
14 E. Fargin, I. Bussereau, G. Le Flem, R. Olazcuaga, C. Cartier and H. Dexpert, *Eur. J. Inorg. Solid State Chem.*, in the press.
15 I. Bussereau, Thesis, University of Bordeaux I, 1991.
16 W. L. Wanmaker and H. L. Spier, *J. Electrochem. Soc., 109* (2) (1962) 109.
17 W. F. Schmid and R. W. Mooney, *J. Electrochem. Soc., 111* (6) (1964) 668.
18 J. Simonetti and D. S. McClure, *Phys. Rev. B, 16* (1977) 3887.
19 C. Pédrini and B. Jacquier, *J. Phys. C, 13* (1980) 4791.
20 H. Chermette and C. Pedrini, *J. Chem. Phys., 75* (1981) 1869.
21 R. L. Chien, J. Simonetti and D. S. McClure, *J. Luminesc., 31/32* (1984) 326.
22 R. Oggioni and P. Scaramelli, *Phys. Status Solidi, 9* (1965) 41.
23 E. Kratzig, T. Timusk and W. Martiensen, *Phys. Status Solidi, 10* (1965) 709.
24 G. Le Pollès, C. Parent, R. Olazcuaga and G. Le Flem, *C.R. Acad. Sci. Paris, 306*, série II (1988) 765.
25 P. Boutinaud, C. Parent, G. Le Flem, B. Moine and C. Pédrini, *J. Phys.: Condensed Matter, 4* (1992) 3031.
26 S. Payne, L. L. Chase and L. A. Boatner, *J. Luminesc., 35* (1986) 171.
27 J. D. Barrie, B. Dunn, G. Hollingsworth and J. I. Zink, *J. Chem. Phys., 93* (1989) 3958.
28 P. K. Mehrotra and R. Hoffmann, *Inorg. Chem., 17* (1978) 2187.
29 E. Eitel, D. Oelkrug, W. Hiller and J. Stähle, *Z. Naturforsch.* Teil B, *35* (1980) 1247.
30 H. D. Hardt and P. Weber, *Z. Anorg. Allg. Chem., 442* (1978) 225.
31 L. G. Deshazer, *Laser Focus, 17* (1981) 22.
32 G. S. Kruglick, G. A. Skripko, A. P. Shkadarevitch, N. Ermolenko, O. G. Gorodetskaya, M. V. Belokon, A. Ashagov and L. E. Zoloterova, *Opt. Spektrosk., 59* (1985) 439.
33 J. C. Zhang, B. Moine, C. Pédrini, C. Parent and G. Le Flem, *J. Phys. Chem. Solids, 51* (1990) 933.
34 P. Boutinaud, E. Duloisy, C. Pédrini, B. Moine, C. Parent and G. Le Flem, *J. Solid State Chem., 94* (1991) 236.
35 J. W. M. Verwey, J. M. Coronado and G. Blasse, *J. Solid State Chem., 92* (1991) 531.
36 S. A. Payne, A. B. Golberg and D. S. McClure, *J. Chem. Phys., 78* (1983) 3668.
37 R. L. Bareman and W. J. Van Sciver, *Phys. Status Solidi B, 46* (1971) 779.